

## LAMINATED COMPOSITES MODELED BY ELEMENTS CORRECTED FOR LOCKING A-PRIORI

João E. Abdalla F<sup>o</sup> <sup>a,b</sup>, Ivan M. Belo<sup>a</sup>, Roberto D. Machado<sup>b</sup>

<sup>a</sup>*Programa de Pós-Graduação em Engenharia Civil, Universidade Tecnológica Federal do Paraná, Av. Sete de Setembro, 3165, 80.215-901, Curitiba, Paraná, Brazil, <http://www.utfpr.edu.br>*

<sup>b</sup>*Programa de Pós-Graduação em Engenharia Mecânica, Pontifícia Universidade Católica do Paraná - PUCPR, R. Imaculada Conceição, 1155, 80.215-901, Curitiba, Paraná, Brazil, <http://www.pucpr.br>*

**Keywords:** Laminated Composites Plates, Finite Elements, Strain Gradient Notation, Shear Locking, Spurious Zero Energy Modes, Parasitic Shear

**Abstract.** An eight node serendipity element free of locking and spurious zero energy modes is formulated to model laminated composite plates. A first-order shear deformation theory and equivalent lamina assumption are adopted. The model represents transverse shear strains and stresses as constants while their actual variations are parabolic. Thus, a shear correction factor is used. Strain gradient notation is employed which allows for a detailed a-priori analysis of the finite element model. Its polynomial expansions are inspected and spurious terms which are responsible for shear locking are identified. The element is corrected by simply removing the spurious terms from those expansions. The compatibility modes are also clearly identified and maintained, preventing the introduction of spurious zero energy modes. Numerical results show locking effects caused by the spurious terms on displacement and transverse stresses solutions. They also show that properly refined meshes composed of corrected elements provide solutions which converge rather well to analytical solutions.

## 1 INTRODUCTION

This paper describes the development of an eight-node serendipity finite element for the analysis of laminated composite plates using strain gradient notation. The element is based on a first-order shear deformation theory, which considers the transverse shear strains according to Mindlin's theory. The equivalent lamina assumption is employed to treat the laminate as one single, orthotropic lamina plate whose constitutive properties are the average of the properties of the constituent laminae.

Strain gradient notation is an alternative notation for writing finite element polynomials. It is a physically interpretable notation which relates displacements to the kinematics quantities of the continuum. The identification of this relationship is possible due to a procedure which identifies the physical contents of the polynomial coefficients (Dow, 1999). The main advantage of the use of strain gradient notation is that the modeling characteristics of the finite element become apparent to the developer since the early steps of the formulation. This allows for sources of modeling errors to be identified and consequently removed from the finite element polynomial expansions for strains prior to the formation of the element stiffness matrix. Sources of shear locking will be precisely identified and removed from the element's strains. Causes of spurious zero energy modes will be explained, and this deficiency will be avoided by correctly eliminating shear locking.

Elimination of locking in finite element analysis of plates and shells has been a major concern for many decades. The related literature is vast and it is not the purpose of this work to make a thorough review. Reference will be made to a few important works which have motivated the research reported in this paper. An early work (Zienkiewicz et al., 1971) recognizes that the serendipity plate element (Ahamad et al., 1970) increases unduly in stiffness for thin problems. Recognizing the phenomenon as parasitic shear, they apply a reduced-order integration scheme (2x2 Gauss quadrature) to calculate transverse shear stresses. Although this procedure represents an improvement over normal integration, the element behaves poorly in the thin plate limit (Hughes et al., 1978).

The regular four-node  $C^0$ -continuity plate element (bilinear element) is employed successfully in the analysis of thin plates when a selective reduced integration is adopted. The 2x2 Gauss quadrature scheme is used to integrate the bending energy while the 1x1 Gauss quadrature scheme is used to integrate the shear energy in order to avoid locking (Hughes et al., 1977).

A follow-up work (Hughes et al., 1978) addresses reduced and selective reduced integration of Lagrange  $C^0$ -continuity plate elements. The authors elect Lagrange elements under the premise that triangles and serendipity quadrilateral elements may behave poorly. Although considerable improvement is achieved in plate analysis through selective reduced integration of Lagrange elements, findings are that those elements are rank deficient. That is, the elements contain spurious zero energy modes.

In order to avoid rank deficiency, the "heterosis" plate bending element (Hughes and Cohen, 1978) is developed. The element is based on Mindlin's plate theory ( $C^0$ -continuity) and it is designed with the purpose of analyzing thick as well as thin plates. The element is a nine-node quadrilateral which employs serendipity shape functions for the transverse displacement, and Lagrange shape functions for the rotations. A selective reduced integration scheme is employed to remove locking. The "heterosis" element possesses correct rank (does not possess spurious zero energy modes), is invariant, and passes the Mindlin's theory plate patch test. Numerical experiments show that the "heterosis" element is superior in the overall sense because it presents neither a divergent behavior nor an oscillating behavior.

Another author (Prathap, 1997) proposes the use of the field-consistency approach to construct well-behaved plate elements. A consistent strain field is constructed from orthogonality relations which are derived from the Hellinger-Reissner theorem. A two-node Timoshenko beam element is constructed in this manner to explain the procedure and to demonstrate the analogy to a displacement-based element integrated using only one Gauss point or to an element formulated using mixed interpolation fields. Further, the author applies the field-consistency approach to construct a quadrilateral four-node Mindlin plate element. The resulting element does not lock and does not present spurious zero energy modes.

A four-node plate bending element based on Mindlin/Reissner theory and mixed interpolation is devised (Bathe and Dvorkin, 1985). The element is a special case of a general nonlinear shell element formulation. Locking is avoided by using different interpolations for bending and transverse shear effects. Specifically, rotations and transverse displacements are interpolated using the natural coordinates bilinear shape functions, and transverse shear strains are interpolated in terms of physical shear strains defined at four intermediate points over the sides of the quadrilateral. The element contains no spurious zero energy modes and does not lock when applied to thin plates.

In this work, spurious terms which are present in the shear strain polynomial expansions of the serendipity plate element are identified by inspection. It is demonstrated both theoretically and numerically that they are flexural terms which cause locking of the model by increasing the element's shear strain energy unduly when the plate undergoes bending. It is also demonstrated that spurious zero energy modes are not introduced into the model by recognizing and not removing the compatibility modes. These can be easily confused with shear locking terms and be inadvertently removed. This is the limitation of reduced-order integration schemes in attempting to correct elements for locking. Along with eliminating legitimate spurious terms responsible for locking, those techniques also eliminate compatibility modes, thus introducing spurious zero energy modes. Strain gradient notation allows for the clear identification of the compatibility modes and legitimate spurious terms in the element's formulation. The transparency of strain gradient notation offers a simple and free-of-drawbacks means to deal with spurious terms. The element is corrected for locking by simply removing the spurious terms from the shear strains expressions. As the compatibility modes are maintained, spurious zero energy modes are not introduced. Thus, the strain gradient notation element has the advantages that locking is taken care of correctly and *a-priori* of the formation of the stiffness matrix and of the computer implementation, and that it is of correct rank.

Research on modeling and analysis of laminated composite structures has increased significantly in the last three decades. The concern to accurately represent the actual behavior of this kind of structures has led researchers to develop analytical and numerical models every time more refined. A thorough review on theories and computational models for laminated composites has been presented (Reddy and Averill, 1991) and further updated (Reddy, 2004). Another thorough review on theories for isotropic and anisotropic laminated plates has been conducted which cites over four hundred references (Ghugal and Shimpi, 2002).

Several works have proposed high-order deformation theories to model laminated composite plates (Lo et al., 1977a,b; Singh and Rao, 1995; Bose and Reddy, 1998a,b). An overview of the relationships between classical and shear deformation theories has been presented (Reddy and Wang, 2000). Computational models ranging from simple to refined have been developed to perform numerical evaluation of all those theories (Bose and Reddy, 1998b; Reddy, 1989). Further advances include a layerwise model that avoids shear locking by employing a transverse shear deformation field which is compatible with the assumed displacement field (Botello et al., 1999). Also, a four-noded mixed finite element for composites is developed which is based on the work of Bathe and Dvorkin (Brank and

Carrera, 2000). A triangular element for composites which is free of locking and spurious zero energy modes is developed (Sheikh and Chakrabarti, 2003) based on Reddy's simple higher-order shear deformation theory. Further, Reddy's displacement for third order shear deformation theory is employed to derive a set of equations to model the behavior of laminated plates, and a triangular finite element is implemented using those equations (Aagaah, 2003).

Although recognizing important advances in the numerical analysis of laminated composites using more refined theories (some mentioned above), the authors of this paper adopt a first-order shear deformation theory in the formulation of this serendipity plate element. The element is implemented in a FORTRAN finite element code in two versions; namely, one containing the spurious terms and other after elimination of the spurious terms. In order to assess the performance of the element and to validate the procedure of eliminating the sources of locking, solutions provided by both versions of the element are compared. Comparison of numerical results shows the manifestation of shear locking and attenuation of its effects provided by mesh refinement. Numerical results also demonstrate that removal of the spurious terms eliminates shear locking. Furthermore, the corrected model is validated by comparing numerical solutions with results obtained from analytical solutions (Reddy, 2004). This work demonstrates that the element presented provides accurate results and converges quickly to the correct solution after spurious terms which are responsible for shear locking are eliminated.

## 2 THEORETICAL BACKGROUND

The kinematics relations according to the Mindlin or first-order plate theory may be written as follows:

$$u(x, y, z) = u_o(x, y) + z\theta_x(x, y) \quad (1)$$

$$v(x, y, z) = v_o(x, y) - z\theta_y(x, y) \quad (2)$$

$$w(x, y) = w \quad (3)$$

$$\theta_x(x, y) = \frac{\partial u(x, y, z)}{\partial z} \quad (4)$$

$$\theta_y(x, y) = -\frac{\partial v(x, y, z)}{\partial z} \quad (5)$$

where  $u$  and  $v$  are in-plane displacements along the  $x$  and  $y$  directions, respectively,  $w$  is the out-of-plane (normal to the middle surface) displacement,  $\theta_x$  and  $\theta_y$  are rotations in the  $x$  and  $y$  directions, respectively (or around the  $y$  and  $x$  axes, respectively), and  $u_o$  and  $v_o$  are the middle surface's in-plane displacements along the  $x$  and  $y$  directions, respectively. The displacement  $w$  is independent of rotations, which allows transverse shear deformation representation. This feature is particularly important for modeling thick plates and laminated composites.

Strains are defined as follows:

$$\begin{Bmatrix} \varepsilon_x \\ \varepsilon_y \\ \gamma_{xy} \\ \gamma_{yz} \\ \gamma_{xz} \end{Bmatrix} = \begin{Bmatrix} u_{0,x} \\ v_{0,y} \\ u_{0,y} + v_{0,x} \\ 0 \\ 0 \end{Bmatrix} + \begin{Bmatrix} z\theta_{x,x} \\ -z\theta_{y,y} \\ z(\theta_{x,y} - \theta_{y,x}) \\ w_{,y} - \theta_y \\ w_{,x} + \theta_x \end{Bmatrix} \quad (6)$$

where the first vector contains membrane strains and the second vector contains plate bending strains.

The strain energy of the laminate is the sum of the strain energies of its laminae. Hence,

$$U = \frac{1}{2} \sum_{k=1}^n \int_{\Omega_k} \{\varepsilon\}_k^T [Q]_k \{\varepsilon\}_k d\Omega_k \quad (7)$$

where  $k$  is a typical lamina,  $n$  is the total number of laminae,  $\{\varepsilon\}_k$  is the strain vector of lamina  $k$ ,  $[Q]_k$  is the constitutive properties matrix of lamina  $k$ , and  $\Omega_k$  is the volume of lamina  $k$ .

Strain gradient notation is mainly characterized by relating displacements and strains to the kinematics quantities of the continuum in a way which is transparent to the analyst (Dow, 1999). The referred kinematics quantities are rigid body modes, strains, and first-order and higher-order derivatives of strains, and they are generally referred to as *strain gradients*. The relations of displacements and strains to strain gradients are given in symbolic form, respectively, by:

$$\{d\} = [\phi] \{\varepsilon_{sg}\} \quad (8)$$

$$\{\varepsilon\} = [T_{sg}] \{\varepsilon_{sg}\} \quad (9)$$

where  $[\phi]$  and  $[T_{sg}]$  are the corresponding transformation matrices, and  $\{\varepsilon_{sg}\}$  is the strain gradients vector. This vector contains the set of independent deformation modes that the model is capable of representing. Matrix  $[\phi]$  is comprised of linearly independent vectors, each associated to a strain gradient component, describing a specific deformation pattern of the model. Eq. (8) and Eq. (9) are combined to eliminate vector  $\{\varepsilon_{sg}\}$ , and the resulting expression is substituted into Eq. (7) to yield:

$$U = \frac{1}{2} \{d\}^T [\phi]^{-T} \left( \sum_{k=1}^n \int_{\Omega_k} [T_{sg}]_k^T [Q]_k [T_{sg}]_k d\Omega_k \right) [\phi]^{-1} \{d\} \quad (10)$$

which is an expression of the strain energy for laminated composites in *strain gradient notation*. The quantity between parentheses is called strain energy matrix and it is represented by  $[U_M]$ . The elements of its principal diagonal contain the quantities of strain energy associated with the pure strain modes of the laminate. The other elements of the matrix contain the quantities of energy associated with the coupling between the various strain modes. Matrix  $[U_M]$  may be written as:

$$[U_M] = \int_A \sum_{k=1}^n \int_{Z_{k-1}}^{Z_k} [T_{sg}]_k^T [Q]_k [T_{sg}]_k dZ_k dA \quad (11)$$

where the volume integral has been broken into an integral over the area of the middle surface of the laminate and an integral over its thickness. This line integral is carried out as the sum of the integrals over the thicknesses of the various laminae. The integration limits  $z_{k-1}$  e  $z_k$  represent the bottom and top coordinates of a typical lamina  $k$ , respectively. The integration over the thickness of the laminate yields its stiffness quantities:

$$A_{ij} = \sum_{k=1}^n (Q_{ij})_k (Z_k - Z_{k-1}) \quad (12)$$

$$B_{ij} = \frac{1}{2} \sum_{k=1}^n (Q_{ij})_k (Z_k^2 - Z_{k-1}^2) \quad (13)$$

$$D_{ij} = \frac{1}{3} \sum_{k=1}^n (Q_{ij})_k (Z_k^3 - Z_{k-1}^3) \quad (14)$$

$$A_{ij}^* = K \sum_{k=1}^n (Q_{ij})_k (Z_k - Z_{k-1}) \quad (15)$$

where  $A$  is the membrane stiffness,  $B$  is the membrane-bending coupling stiffness,  $D$  is the bending stiffness, and  $A^*$  is the transverse shear stiffness and it is subjected to a shear correction factor  $K$ . The determination of the shear correction factor for laminates is still an open issue as it depends on lamination scheme, geometry, and material properties (Reddy, 2004). The value  $5/6$ , which is very accurate for homogeneous, isotropic plates, is most commonly used. This value is adopted in the numerical analyses performed in this paper to allow for comparisons to the analytical solutions employed as reference solutions (Reddy, 2004).

Finally, as the strain energy in terms of the stiffness matrix is given by:

$$U = \frac{1}{2} \{d\}^T [K] \{d\} \quad (16)$$

the general expression of the stiffness matrix in strain gradient notation turns out to be:

$$[K] = [\phi]^{-T} [U_M] [\phi]^{-1} \quad (17)$$

### 3 STRAIN GRADIENT NOTATION SERENDIPITY PLATE ELEMENT

The formulation of an eight-node serendipity plate finite element in strain gradient notation is presented in this section. The finite element is shown in figure 1. Five degrees of freedom are associated to each node; namely, in-plane displacements  $u_o$  and  $v_o$ , the out-of-plane displacement  $w$ , and rotations  $\theta_x$  and  $\theta_y$ .

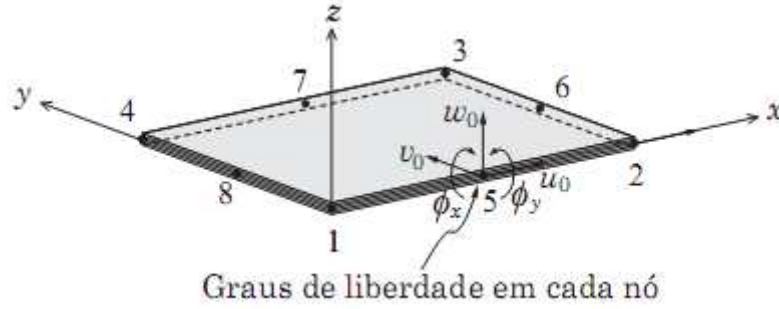


Fig. 1 - Eight-node serendipity plate element.

The displacement polynomial expansions in strain gradient notation, according to Eq.(1) through Eq.(5), are obtained by substituting the unknown coefficients by their physical contents. The procedure to identify physical contents of finite element displacement polynomials is described in detailed by Dow (1999). The strain gradient notation displacement polynomials for this element are presented below:

$$\begin{aligned}
 u(x, y, z) = & (u)_o + (\varepsilon_x)_o x + (\gamma_{xy} / 2 - r)_o y + (\varepsilon_{x,x})_o x^2 / 2 + (\varepsilon_{x,y})_o xy + (\gamma_{xy,y} / 2 - \varepsilon_{y,x})_o y^2 / 2 \\
 & + (\varepsilon_{x,xy})_o x^2 y / 2 + (\varepsilon_{x,yy})_o xy^2 / 2 + (\theta_x + \gamma_{xz} / 2)_o z + (\varepsilon_{x,z})_o xz + (\gamma_{xy,z} - \gamma_{yz,x} + \gamma_{xz,y})_o yz / 2 \\
 & + (\varepsilon_{x,xz})_o x^2 z / 2 + (\gamma_{xy,yz} - \varepsilon_{y,xz})_o y^2 z / 2 + (\varepsilon_{x,yz})_o xyz + (\varepsilon_{x,xyz})_o x^2 yz / 2 + (\varepsilon_{x,yyz})_o xy^2 z / 2
 \end{aligned} \tag{18}$$

$$\begin{aligned}
 v(x, y, z) = & (v)_o + (\gamma_{xy} / 2 + r)_o x + (\varepsilon_y)_o y + (\gamma_{xy,x} - \varepsilon_{x,y})_o x^2 / 2 + (\varepsilon_{y,x})_o xy + (\varepsilon_{y,y})_o y^2 / 2 \\
 & + (\varepsilon_{y,xx})_o x^2 y / 2 + (\varepsilon_{y,xy})_o xy^2 / 2 + (\gamma_{yz} / 2 - \theta_y)_o z + (\gamma_{xy,z} + \gamma_{yz,x} - \gamma_{xz,y})_o xz / 2 + (\varepsilon_{y,z})_o yz \\
 & + (\gamma_{xy,xz} - \varepsilon_{x,yz})_o x^2 z / 2 + (\varepsilon_{y,yz})_o y^2 z / 2 + (\varepsilon_{y,xz})_o xyz + (\varepsilon_{y,xxz})_o x^2 yz / 2 + (\varepsilon_{y,xyz})_o xy^2 z / 2
 \end{aligned} \tag{19}$$

$$\begin{aligned}
 w(x, y) = & (w)_o + (\gamma_{xz} / 2 - \theta_x)_o x + (\gamma_{yz} / 2 + \theta_y)_o y + (\gamma_{xz,x} - \varepsilon_{x,z})_o x^2 / 2 \\
 & + (-\gamma_{xy,z} + \gamma_{yz,x} + \gamma_{xz,y})_o xy / 2 + (\gamma_{yz,y} - \varepsilon_{y,z})_o y^2 / 2 + (\gamma_{xz,xy} - \varepsilon_{x,yz})_o x^2 y / 2 \\
 & + (\gamma_{yz,xy} - \varepsilon_{y,xz})_o y^2 x / 2
 \end{aligned} \tag{20}$$

$$\begin{aligned}
 \theta_x(x, y) = & (\theta_x + \gamma_{xz} / 2)_o + (\varepsilon_{x,z})_o x + (\gamma_{xy,z} - \gamma_{yz,x} + \gamma_{xz,y})_o y / 2 \\
 & + (\varepsilon_{x,xz})_o x^2 / 2 + (\gamma_{xy,yz} - \varepsilon_{y,xz})_o y^2 / 2 + (\varepsilon_{x,yz})_o xy + (\varepsilon_{x,xyz})_o x^2 y / 2 + (\varepsilon_{x,yyz})_o xy^2 / 2
 \end{aligned} \tag{21}$$

$$\begin{aligned}
 \theta_y(x, y) = & -(\gamma_{yz} / 2 - \theta_y)_o - (\gamma_{xy,z} + \gamma_{yz,x} - \gamma_{xz,y})_o x / 2 - (\varepsilon_{y,z})_o y \\
 & - (\gamma_{xy,xz} - \varepsilon_{x,yz})_o x^2 / 2 - (\varepsilon_{y,yz})_o y^2 / 2 - (\varepsilon_{y,xz})_o xy - (\varepsilon_{y,xxz})_o x^2 y / 2 - (\varepsilon_{y,xyz})_o xy^2 / 2
 \end{aligned} \tag{22}$$

These expansions contain the set of fourty strain states that the element is capable of representing. These strain states are rigid body modes, constant strains, flexural strains and shear strains gradients, which are listed below:

- |                   |   |
|-------------------|---|
| Rigid body modes: | $(u)_o (v)_o (r)_o (w)_o (\theta_x)_o (\theta_y)_o$   |
| Constant strains: | $(\varepsilon_x)_o (\varepsilon_y)_o (\gamma_{xy})_o (\gamma_{xz})_o (\gamma_{yz})_o$                             |
| Flexural strains: | $(\varepsilon_{x,x})_o (\varepsilon_{x,y})_o (\varepsilon_{x,z})_o (\varepsilon_{x,xy})_o (\varepsilon_{x,yy})_o$ |

$$\begin{aligned}
& \left( \varepsilon_{x,xz} \right)_o \left( \varepsilon_{x,yz} \right)_o \left( \varepsilon_{x,xyz} \right)_o \left( \varepsilon_{x,yyz} \right)_o \\
& \left( \varepsilon_{y,x} \right)_o \left( \varepsilon_{y,y} \right)_o \left( \varepsilon_{y,z} \right)_o \left( \varepsilon_{y,xy} \right)_o \left( \varepsilon_{y,xz} \right)_o \\
& \left( \varepsilon_{y,xx} \right)_o \left( \varepsilon_{y,yz} \right)_o \left( \varepsilon_{y,xxz} \right)_o \left( \varepsilon_{y,xyz} \right)_o \\
\text{Shear strain gradients:} & \left( \gamma_{xy,x} \right)_o \left( \gamma_{xy,y} \right)_o \left( \gamma_{xy,z} \right)_o \\
& \left( \gamma_{xy,xz} \right)_o \left( \gamma_{xy,yz} \right)_o \left( \gamma_{xz,x} \right)_o \left( \gamma_{xz,y} \right)_o \\
& \left( \gamma_{xz,xy} \right)_o \left( \gamma_{yz,x} \right)_o \left( \gamma_{yz,y} \right)_o \left( \gamma_{yz,xy} \right)_o
\end{aligned}$$

The elastic strain expansions for the element are obtained through application of Eq.(6):

$$\begin{aligned}
\varepsilon_x = & \left( \varepsilon_x \right)_o + \left( \varepsilon_{x,x} \right)_o x + \left( \varepsilon_{x,y} \right)_o y + \left( \varepsilon_{x,yy} \right)_o y^2 / 2 + \left( \varepsilon_{x,z} \right)_o z \\
& + \left( \varepsilon_{x,xz} \right)_o xz + \left( \varepsilon_{x,yz} \right)_o yz + \left( \varepsilon_{x,xyz} \right)_o xyz + \left( \varepsilon_{x,yyz} \right)_o y^2 z / 2
\end{aligned} \quad (23)$$

$$\begin{aligned}
\varepsilon_y = & \left( \varepsilon_y \right)_o + \left( \varepsilon_{y,x} \right)_o x + \left( \varepsilon_{y,y} \right)_o y + \left( \varepsilon_{y,xx} \right)_o x^2 / 2 + \left( \varepsilon_{y,xy} \right)_o xy + \left( \varepsilon_{y,z} \right)_o z \\
& + \left( \varepsilon_{y,yz} \right)_o yz + \left( \varepsilon_{y,xz} \right)_o xz + \left( \varepsilon_{y,xxz} \right)_o x^2 z / 2 + \left( \varepsilon_{y,xyz} \right)_o xyz
\end{aligned} \quad (24)$$

$$\begin{aligned}
\gamma_{xy} = & \left( \gamma_{xy} \right)_o + \left( \gamma_{xy,x} \right)_o x + \left( \gamma_{xy,y} \right)_o y + \left( \gamma_{xy,z} \right)_o z + \left( \gamma_{xy,xz} \right)_o xz + \left( \gamma_{xy,yz} \right)_o yz \\
& + \left( \varepsilon_{x,xy} \right)_o x^2 / 2 + \left( \varepsilon_{x,yy} + \varepsilon_{y,xx} \right)_o xy + \left( \varepsilon_{y,xy} \right)_o y^2 / 2 + \left( \varepsilon_{x,xyz} \right)_o x^2 z / 2 \\
& + \left( \varepsilon_{x,yyz} + \varepsilon_{y,xxz} \right)_o xyz + \left( \varepsilon_{y,xyz} \right)_o y^2 z / 2
\end{aligned} \quad (25)$$

$$\begin{aligned}
\gamma_{yz} = & \left( \gamma_{yz} \right)_o + \left( \gamma_{yz,x} \right)_o x + \left( \gamma_{yz,y} \right)_o y + \left( \gamma_{yz,xy} \right)_o xy + \left( \gamma_{xy,xz} \right)_o x^2 / 2 + \left( \gamma_{xz,xy} \right)_o x^2 / 2 \\
& - \left( \varepsilon_{x,yz} \right)_o x^2 + \left( \varepsilon_{y,yz} \right)_o y^2 / 2 + \left( \varepsilon_{y,xxz} \right)_o x^2 y / 2 + \left( \varepsilon_{y,xyz} \right)_o xy^2 / 2
\end{aligned} \quad (26)$$

$$\begin{aligned}
\gamma_{xz} = & \left( \gamma_{xz} \right)_o + \left( \gamma_{xz,x} \right)_o x + \left( \gamma_{xz,y} \right)_o y + \left( \gamma_{xz,xy} \right)_o xy + \left( \gamma_{xy,yz} \right)_o y^2 / 2 + \left( \gamma_{yz,xy} \right)_o y^2 / 2 \\
& + \left( \varepsilon_{x,xz} \right)_o x^2 / 2 - \left( \varepsilon_{y,xz} \right)_o y^2 + \left( \varepsilon_{x,xyz} \right)_o x^2 y / 2 + \left( \varepsilon_{x,yyz} \right)_o xy^2 / 2
\end{aligned} \quad (27)$$

Examination of these strains expressions will reveal the presence of spurious terms *a-priori*. Strains expansions should be only composed of terms which are physically related to the strains quantities they represent. Examination of the expansions for normal strains, Eq.(23) and Eq.(24), shows that all coefficients are associated to their respective normal strains. Therefore, all those terms are legitimate as they correctly contribute to the representation of normal strains.

However, examination of the expansions for shear strains, Eq.(25), Eq.(26) and Eq.(27), reveals that besides legitimate terms, these expansions contain terms which are related to normal strains. In general, normal strain terms in shear strains expansions are spurious terms because they will increase the shear strain energy of the element unduly when activated during deformation. That is, they will cause shear locking.

Spurious terms are introduced due to the use of incompatible displacement polynomials. In the present case, the membrane displacement polynomials selected are incomplete, third order polynomials. They do not contain the terms  $x^3$  and  $y^3$ . This causes the presence of spurious terms in the in-plane shear strain expansion  $\gamma_{xy}$ . Further, the order of the rotation polynomial expansions and the order of the out-of-plane displacement polynomial expansion are the same, which is inconsistent with Mindlin plate theory. The reason is that the transverse shear strains are defined as the sum of the rotations and the first derivatives of the out-of-plane displacement



(see Eq.(6)). These polynomials would be consistent if the out-of-plane displacement polynomial were one order higher than the order of the rotation polynomials. It is this inconsistency that causes the presence of spurious terms in the transverse shear strain expansions  $\gamma_{yz}$  and  $\gamma_{xz}$ .

Based on these arguments, after examining the strain expansions above, one might be tempted to remove all the normal strain gradient terms from the shear strain expansions to produce a well-formulated element. However, careful scrutiny of the shear strain expansions reveals that not all their normal strain gradient terms are spurious. Some are actually terms that are needed by the element. Such terms are necessary as they are recognized as the terms of compatibility equations of the elasticity theory. That is, they are compatible modes. This will be shown in the following for each shear strain expansion.

The expansion of the in-plane shear strain  $\gamma_{xy}$ , Eq.(25), contains eight normal strain gradient terms. Four of these terms are needed in the formulation because they give rise to the following compatibility equations:

$$\gamma_{xy,xy} = \varepsilon_{x,yy} + \varepsilon_{y,xx} \quad (28)$$

$$\gamma_{xy,xyz} = \varepsilon_{x,yyz} + \varepsilon_{y,xxz} \quad (29)$$

and, hence, the only spurious terms present in the in-plane shear strain expansion are

$$\left(\varepsilon_{x,xy}\right)_o, \left(\varepsilon_{y,xy}\right)_o, \left(\varepsilon_{x,xyz}\right)_o, \left(\varepsilon_{y,xyz}\right)_o.$$

Proceeding on with the *a-priori* analysis, it is seen that the expansion of the transverse shear strain  $\gamma_{yz}$ , Eq.(26), contains four normal strain gradient terms, one gradient of the in-plane shear strain and one gradient of the transverse shear strain in the plane X-Z, which appear to be spurious for not belonging to the Taylor series expansion of  $\gamma_{yz}$ . However, according to the following compatibility equation:

$$\gamma_{yz,xx} = \gamma_{xy,xz} + \gamma_{xz,xy} - 2\varepsilon_{x,yz} \quad (30)$$

the only spurious terms are  $\left(\varepsilon_{y,yz}\right)_o$ ,  $\left(\varepsilon_{y,xxz}\right)_o$ , and  $\left(\varepsilon_{y,xyz}\right)_o$ .

Finally, it is seen that in the expansion of the transverse shear strain  $\gamma_{xz}$ , Eq.(27), there are four normal strain gradient terms, one gradient of the in-plane shear strain, and one gradient of the transverse shear strain in the plane Y-Z, which appear to be alien to the expansion. However, according to the following compatibility equation:

$$\gamma_{xz,yy} = \gamma_{xy,yz} + \gamma_{yz,xy} - 2\varepsilon_{y,xz} \quad (31)$$

the only spurious terms are  $\left(\varepsilon_{x,xz}\right)_o$ ,  $\left(\varepsilon_{x,xyz}\right)_o$ , and  $\left(\varepsilon_{x,yyz}\right)_o$ .

The terms on the left-hand sides of the compatibility equations above belong to the Taylor series expansions of the corresponding shear strains. Consequently, the terms on the right-hand sides of those equations are compatible modes. Thus, those terms must be kept, and the only terms to be eliminated are those recognized as spurious terms. Proceeding on with the elimination results on the corrected shear strain expansions, which are:

$$\begin{aligned} \gamma_{xy} = & \left(\gamma_{xy}\right)_o + \left(\gamma_{xy,x}\right)_o x + \left(\gamma_{xy,y}\right)_o y + \left(\gamma_{xy,z}\right)_o z + \left(\gamma_{xy,xz}\right)_o xz + \left(\gamma_{xy,yz}\right)_o yz \\ & + \left(\varepsilon_{x,yy} + \varepsilon_{y,xx}\right)_o xy + \left(\varepsilon_{x,yyz} + \varepsilon_{y,xxz}\right)_o xyz \end{aligned} \quad (32)$$

$$\gamma_{yz} = (\gamma_{yz})_o + (\gamma_{yz,x})_o x + (\gamma_{yz,y})_o y + (\gamma_{yz,xy})_o xy + (\gamma_{xy,xz})_o x^2 / 2 + (\gamma_{xz,xy})_o x^2 / 2 - (\epsilon_{x,yz})_o x^2 \quad (33)$$

$$\gamma_{xz} = (\gamma_{xz})_o + (\gamma_{xz,x})_o x + (\gamma_{xz,y})_o y + (\gamma_{xz,xy})_o xy + (\gamma_{xy,yz})_o y^2 / 2 + (\gamma_{yz,xy})_o y^2 / 2 - (\epsilon_{y,xz})_o y^2 \quad (34)$$

These shear strain expansions do not contain any spurious terms and the compatible modes have been kept. Removal of the spurious terms ensures that shear locking will not occur, and the presence of the compatible modes prevents the introduction of spurious zero energy modes. Therefore, these two measures must be taken to guarantee that spurious mechanisms will not occur in the eight-node serendipity plate element during analysis. As all spurious terms are present in shear strains polynomials, they may be referred to as parasitic shear terms as it has been done in the literature (Dow, 1999; Zienkiewicz et al., 1970).

The eight-node plate element developed above will be validated in the next section through comparison of numerical and analytical results of selected problems. Also, the effects of the identified spurious terms on the behavior of the element will be investigated.

## 4 NUMERICAL APPLICATIONS

In this section, two laminated composite plate problems are analyzed employing the serendipity plate model described above.

### 4.1 Application #1

To start, a cantilever plate problem is analyzed which demonstrates with great clarity the severe shear locking caused by the spurious terms present in the eight-node serendipity plate element. The plate is a two-layer angle ply laminate with lamination scheme  $-45^\circ/+45^\circ$  subjected to two point loads applied at the corners of the free end. Fig. 2 shows the lay-out of this problem.

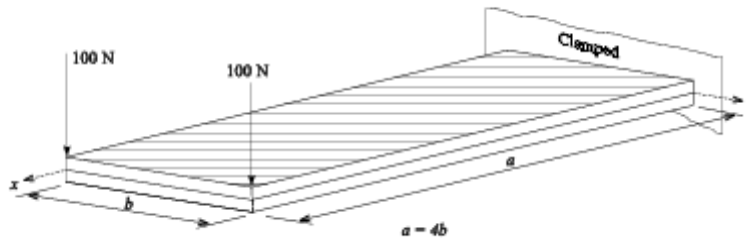


Fig. 2 - Cantilever plate subjected to concentrated loads at the free-end. Anti-symmetric angle-ply laminate -  $45^\circ/+45^\circ$ . Problem definition.

Fig. 3(a) and Fig. 3(b) show the transverse displacement  $w$  solutions of the plate modeled with elements containing the spurious terms and elements corrected for the spurious terms, respectively. It is seen that the former is much stiffer than the latter, evidencing the strong shear locking effect. According to these figures, the maximum displacements calculated for both models are 0.08 m and 0.18 m, respectively. Therefore, it is apparent that shear locking causes the solution to be greatly underestimated. Fig. 3(c) shows the behaviors of the two models with mesh refinement. The solutions without spurious terms converge asymptotically and very rapidly.

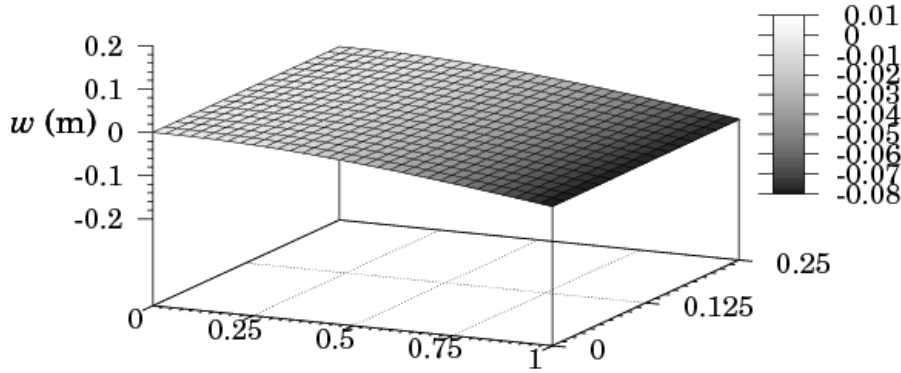


Fig. 3(a) - Cantilever plate subjected to concentrated loads at the free-end. Anti-symmetric angle-ply laminate -  $45^\circ/+45^\circ$ . Transverse displacement solutions with spurious terms.

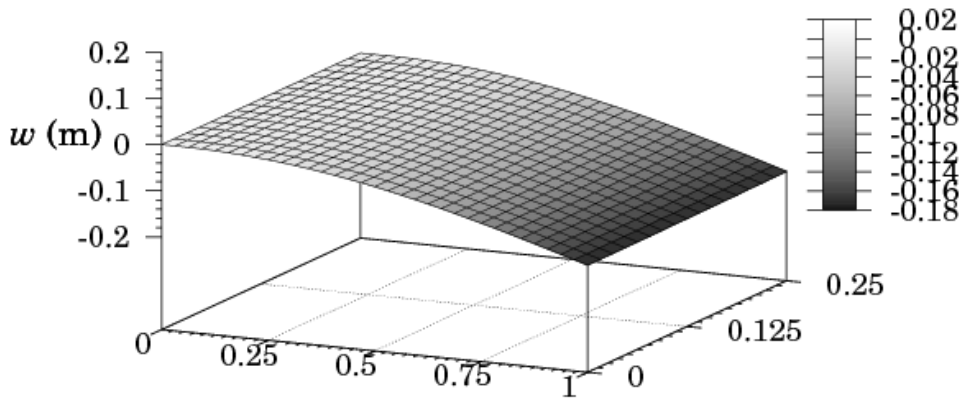


Fig. 3(b) - Cantilever plate subjected to concentrated loads at the free-end. Anti-symmetric angle-ply laminate -  $45^\circ/+45^\circ$ . Transverse displacement solutions without spurious terms.

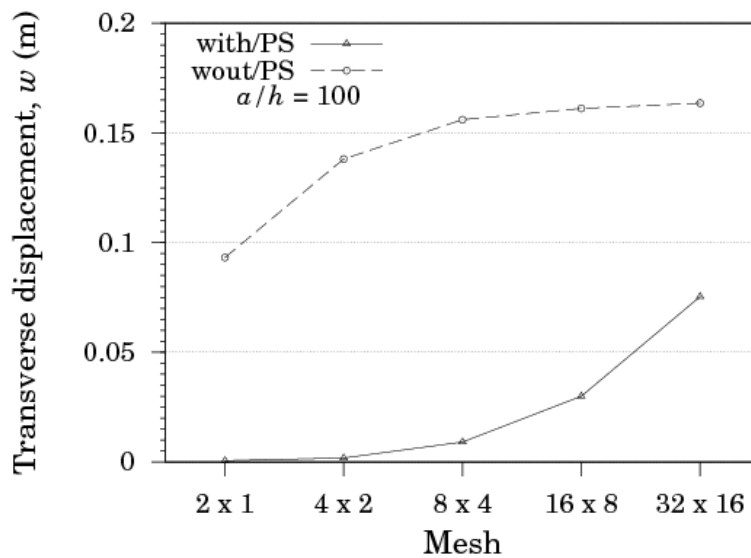


Fig. 3(c) - Cantilever plate subjected to concentrated loads at the free-end. Anti-symmetric angle-ply laminate -  $45^\circ/+45^\circ$ . Convergence of transverse displacement solutions with and without spurious terms.

## 4.2 Application #2

The second application problem is a square simply supported (SS1 supports) cross-ply laminated composite plate subjected to a uniform load of value  $q_0 = 10 \text{ N/m}^2$ . The laminate is symmetric with lamination scheme  $0^\circ/90^\circ/0^\circ$ , and the sides of the laminate are 1.0 m in length ( $a = b = 1.0 \text{ m}$ ) as shown in Fig. 4. The plate is solved both with side length-to-thickness ratios  $a/h = 10$  and  $a/h = 100$ . In-plane normal stresses  $\sigma_{xx}$  and  $\sigma_{yy}$  are calculated at the center point of the plate, while transverse shear stresses  $\tau_{xz}$  and  $\tau_{yz}$  are calculated at borders middle points. Table 1 contains the highest percent error in each solution.

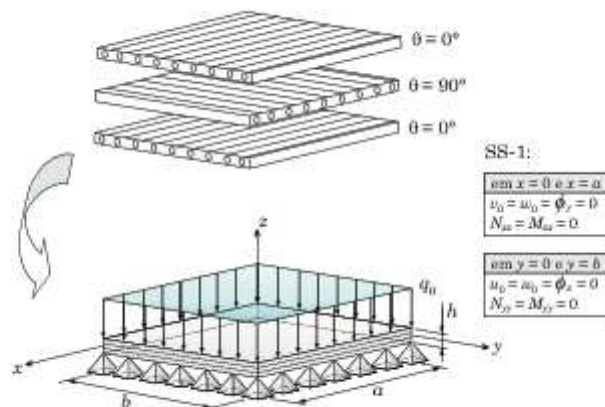


Fig. 4 – Square simply-supported (SS1 boundary conditions) plate subjected to a uniformly distributed load. Symmetric cross-ply laminate  $0^\circ/90^\circ/0^\circ$ . Problem definition.

First, solutions for the thick plate ( $a/h = 10$ ) are presented. Fig. 5(a) through Fig. 5(c) show the results of these analyses. In general, as depicted by these figures, the effects of shear locking although apparent, are not as significant as they are in thin plates. These deleterious effects appear to be greatly attenuated by mesh refinement.

Fig. 5(a) through Fig. 5(c) show solutions for the transverse shear stresses  $\tau_{xz}$ . It is observed that shear locking effects are stronger in the coarser meshes solutions. The corresponding percent errors are significant. Error for the model with spurious terms is 39.63%. These error drops to 17.51% after the removal of the spurious terms. Further, it is also observed that mesh refinement attenuates shear locking, and that the models converge within acceptable levels of error to the analytical solution. The finer mesh for  $\tau_{xz}$  solutions contains errors of only 1.05% and 0.60%. The convergence plots of Fig. 5(c) show that solutions for transverse shear stresses, with and without spurious terms, converge asymptotically to the analytical solutions from lower bounds.

Next, solutions for the thin plate ( $a/h = 100$ ) are presented. Fig. 6(a) through Fig. 6(f) show the results of these analyses. In general, the results depicted by these figures show that the model containing the spurious terms either has convergence delayed or prevented whereas the model without the spurious terms converges well and quickly to the analytical solutions. Fig. 6(a) shows that the spurious terms delay convergence of the normal stresses  $\sigma_{xx}$ , and that even the finer mesh (16x16) presents results which are still far from the analytical results. Errors range from 93.06% to 14.90%. On the other hand, Fig. 6(b) shows that after the removal of the spurious terms, convergence occurs very quickly and well to the analytical solutions. The highest percent error is only 4.38% and drops to 0.29% with refinement. The convergence plots in Fig. 6(c) help to demonstrate these solutions behaviors.

Fig. 6(d) through Fig. 6(f) show the solutions for the transverse shear stresses  $\tau_{xz}$ . The spurious terms cause a strong delay in convergence as demonstrated in Fig. 6(f). The coarser mesh error is 386.42%, dropping to 158.89%. It is also observed that the coarse mesh produces results which are qualitatively erroneous. After the removal of the spurious terms, as

shown in Fig. 6(e), solutions for transverse shear stress converge rather well to the analytical solution. Errors range from 15.50% to 0.47%. The convergence plot in Fig. 6(f) reinforces these observations.

Furthermore, the convergence plots associated to the solutions without spurious terms show that the numerical solutions tend asymptotically to the analytical solutions. This is an important characteristic which indicates fast convergence rates.

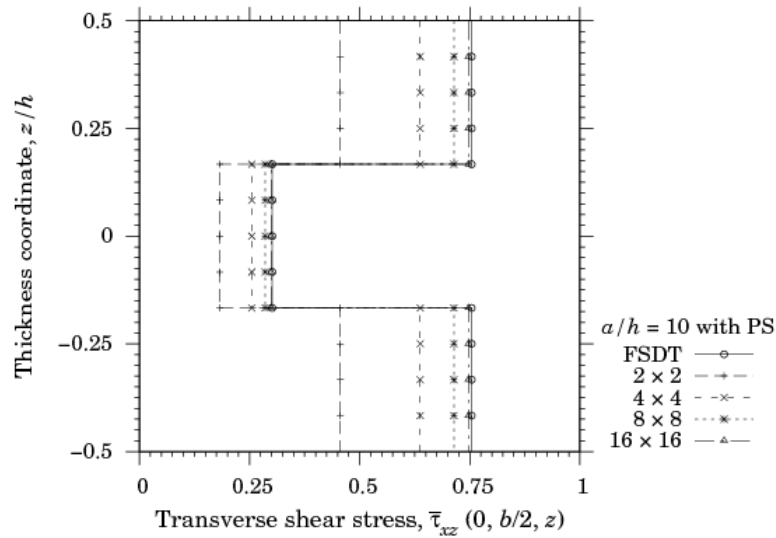


Fig. 5(a) – Square simply-supported (SS1 boundary conditions) plate subjected to a uniformly distributed load with side-to-thickness ratio  $a/h = 10$ . Symmetric cross-ply laminate  $0^{\circ}/90^{\circ}/0^{\circ}$ . Transverse shear stresses  $\tau_{xz}$  computed through the thickness of the laminate with spurious terms.

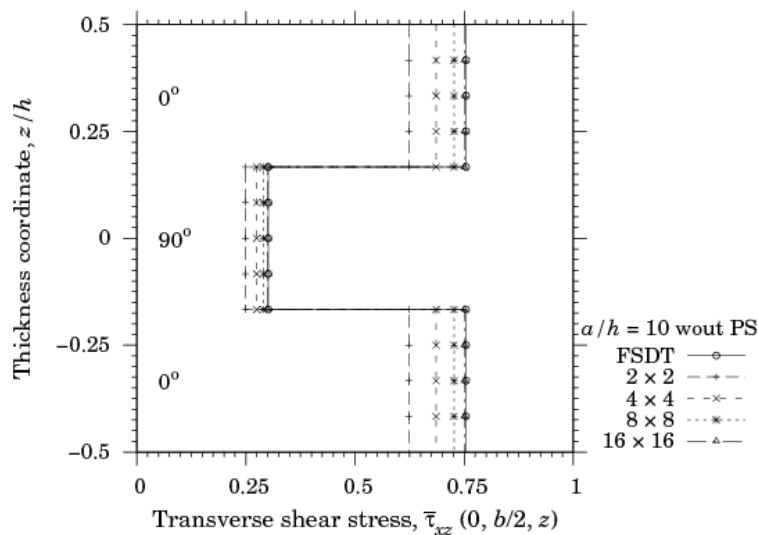


Fig. 5(b) – Square simply-supported (SS1 boundary conditions) plate subjected to a uniformly distributed load with side-to-thickness ratio  $a/h = 10$ . Symmetric cross-ply laminate  $0^{\circ}/90^{\circ}/0^{\circ}$ . Transverse shear stresses  $\tau_{xz}$  computed through the thickness of the laminate without spurious terms.

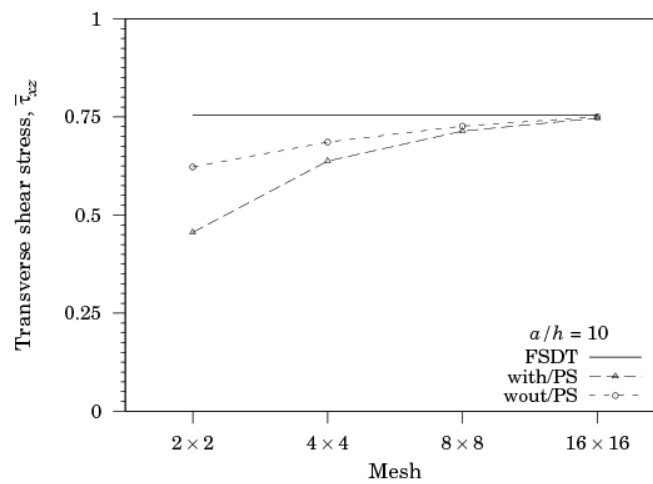


Fig. 5(c) – Square simply-supported (SS1 boundary conditions) plate subjected to a uniformly distributed load with side-to-thickness ratio  $a/h = 10$ . Symmetric cross-ply laminate  $0^\circ/90^\circ/0^\circ$ . Convergence of transverse shear stresses  $\tau_{xz}$  solutions with and without spurious terms.

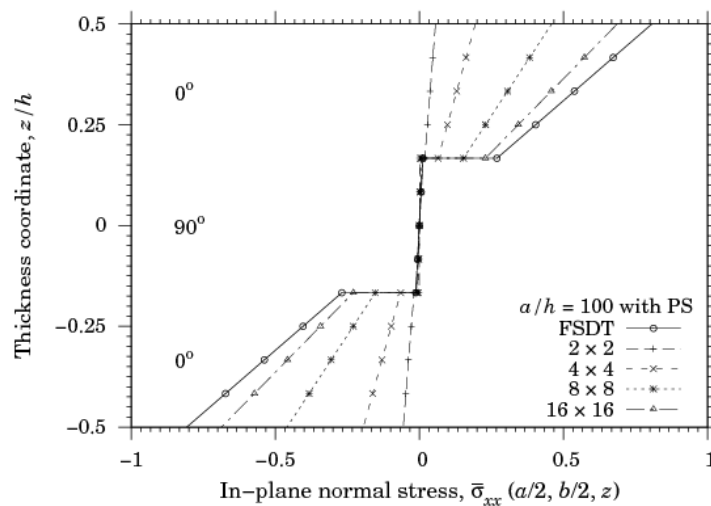


Fig. 6(a) – Square simply-supported (SS1 boundary conditions) plate subjected to a uniformly distributed load with side-to-thickness ratio  $a/h = 100$ . Symmetric cross-ply laminate  $0^\circ/90^\circ/0^\circ$ . Normal stresses  $\sigma_{xx}$  computed through the thickness of the laminate with spurious terms.

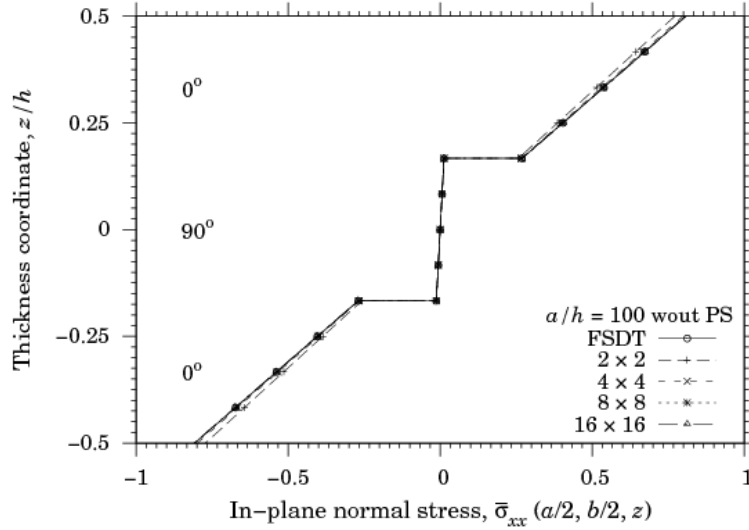


Fig. 6(b) – Square simply-supported (SS1 boundary conditions) plate subjected to a uniformly distributed load with side-to-thickness ratio  $a/h = 100$ . Symmetric cross-ply laminate  $0^\circ/90^\circ/0^\circ$ . Normal stresses  $\sigma_{xx}$  computed through the thickness of the laminate without spurious terms.

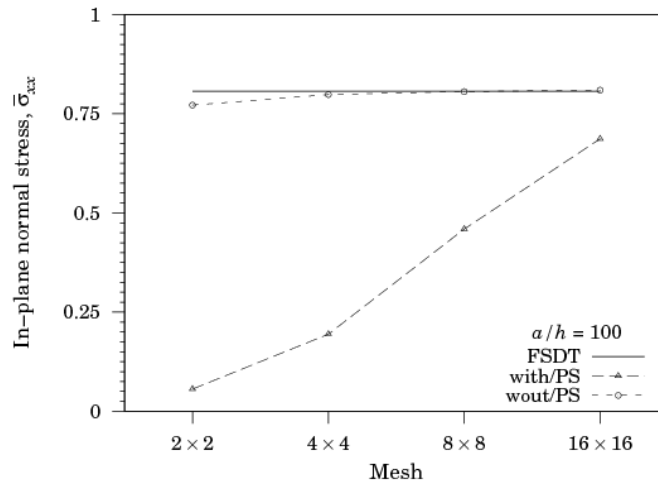


Fig. 6(c) – Square simply-supported (SS1 boundary conditions) plate subjected to a uniformly distributed load with side-to-thickness ratio  $a/h = 100$ . Symmetric cross-ply laminate  $0^\circ/90^\circ/0^\circ$ . Convergence of normal stresses  $\sigma_{xx}$  solutions with and without spurious terms.

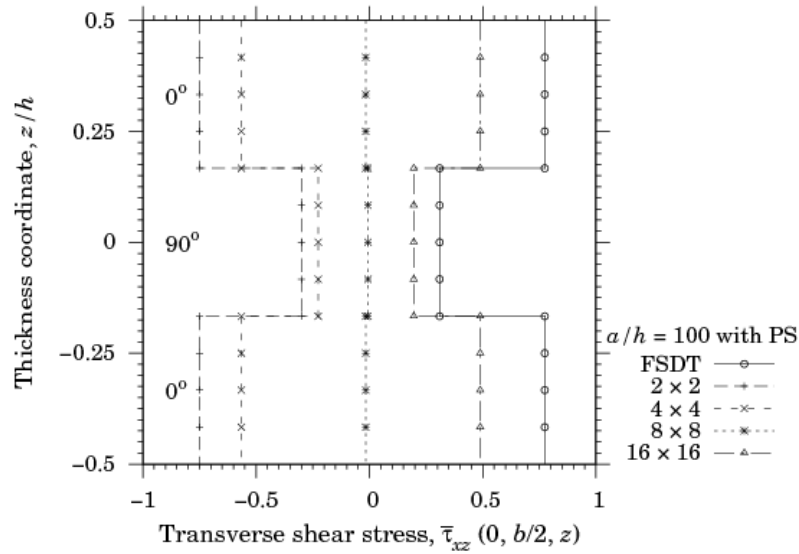


Fig. 6(d) – Square simply-supported (SS1 boundary conditions) plate subjected to a uniformly distributed load with side-to-thickness ratio  $a/h = 100$ . Symmetric cross-ply laminate  $0^\circ/90^\circ/0^\circ$ . Transverse shear stresses  $\tau_{xz}$  computed through the thickness of the laminate with spurious terms.

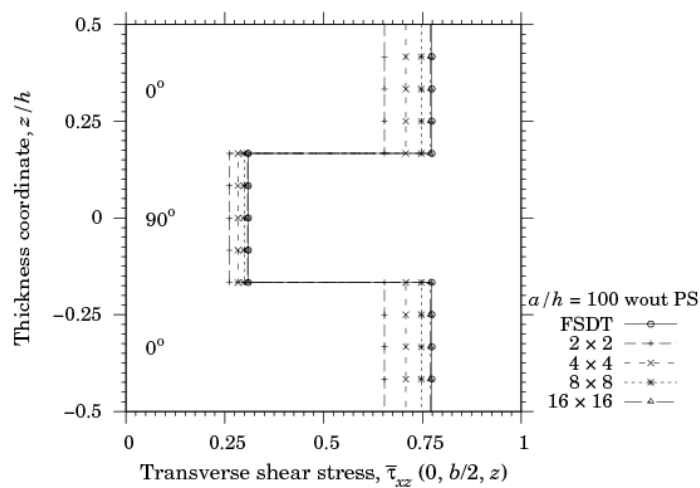


Fig. 6(e) – Square simply-supported (SS1 boundary conditions) plate subjected to a uniformly distributed load with side-to-thickness ratio  $a/h = 100$ . Symmetric cross-ply laminate  $0^\circ/90^\circ/0^\circ$ . Transverse shear stresses  $\tau_{xz}$  computed through the thickness of the laminate without spurious terms.



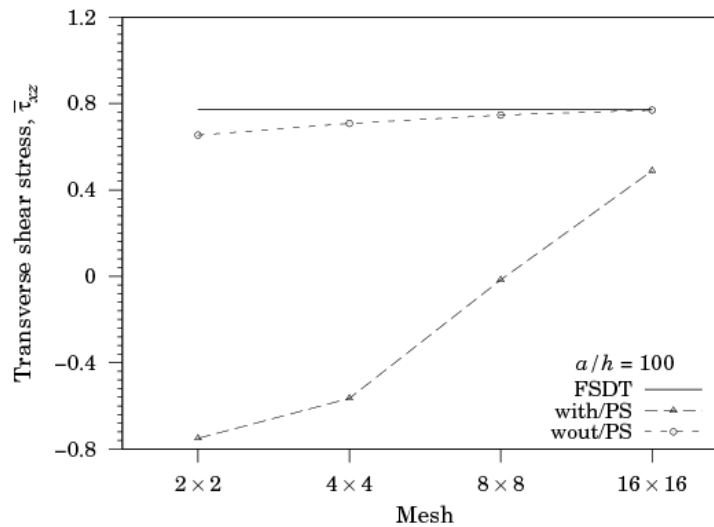


Fig. 6(f) – Square simply-supported (SS1 boundary conditions) plate subjected to a uniformly distributed load with side-to-thickness ratio  $a/h = 100$ . Symmetric cross-ply laminate  $0^\circ/90^\circ/0^\circ$ . Convergence of transverse shear stresses  $\tau_{xz}$  solutions with and without spurious terms.

## 5 CONCLUSION

An eight-node serendipity element has been formulated using strain gradient notation for the analysis laminated composite plates. The shear strains polynomial expansions of the element were inspected for the identification of spurious terms associated to shear locking. Due to the transparency of strain gradient notation, the element has been corrected by simply removing the spurious terms from the shear strains polynomial expansions. In addition, compatible mode terms, which might be mistaken as spurious, have been clearly identified by recognizing that they comprise compatibility equations. Those terms have been retained in order to avoid the introduction of spurious zero energy modes.

Thick and thin rectangular plates have been analyzed for different lamination schemes and boundary conditions. In each case, stresses solutions provided by the model containing the spurious terms have been compared to stresses solutions provided by the corrected model. Those numerical analyses have demonstrated that the identified spurious terms are the cause of shear locking. Those analyses have also demonstrated the effectiveness of the procedure employed to eliminate the spurious terms as, in general, solutions provided by the corrected model converged monotonically and faster to analytical solutions. Further, numerical solutions have shown that mostly transverse shear stresses solutions provided by the model containing the spurious terms might not converge adequately to the correct solutions as the results oscillate or contain great levels of error such as those in Table 1 and Table 2.

A limitation of the current work is that the element has not been designed to assume arbitrary shapes as its formulation does not embed a geometric mapping procedure such as that used in the isoparametric formulation. Nevertheless, it has been shown that the element behaves quite well as a rectangular element after elimination of the spurious terms.

The use of strain gradient notation may be viewed as advantageous as it allows spurious terms responsible for shear locking to be identified and eliminated *a-priori*. The authors claim to have demonstrated theoretically the sources of shear locking and spurious zero energy modes in the eight-node serendipity plate element, and to have built an efficient FSDT element to analyze rectangular laminated composite plates.

**REFERENCES**

- Aagaah MR, Mahinfalah M, Jazar GN. Linear static analysis and finite element modeling for laminated composite plates using third order shear deformation theory. *Composite Structures*, 2003; 62: 27-39.
- Ahamad S, Irons BM, Zienkiewicz OC. Analysis of thick and thin shell structures by curved finite elements. *International Journal for Numerical Methods in Engineering*, 1970; 2: 419-451.
- Bathe KJ, Dvorkin E. A four-node plate bending element based on Mindlin/Reissner plate theory and a mixed interpolation. *International Journal for Numerical Methods in Engineering*, 1985; 21: 367-383.
- Bose P, Reddy JN. Analysis of Composite Plates using various Plate theories, part 1: formulation and analytical solutions. *Structural Engineering and Mechanics*, 1998; 6(6): 583-612.
- Bose P, Reddy JN. Analysis of Composite Plates using various Plate theories, part 2: Finite Element Model and Numerical Results. *Structural Engineering and Mechanics*, 1998; 6(7): 727-746.
- Botello S, Onate E, Canet JM. A layer-wise triangle for analysis of laminated composite plates and shells. *Computers and Structures*, 1999; 70: 635-646.
- Brank B, Carrera E. A family of shear-deformable shell finite elements for composite structures. *Computers and Structures*, 2000; 76: 287-297.
- Dow JO. *A Unified Approach to the Finite Element Method and Error Analysis Procedures*, San Diego, CA: Academic Press, 1999.
- Ghugal YM, Shimpi RP. A Review of Refined Shear Deformation Theories of Isotropic and Anisotropic Laminated Plates. *Journal of Reinforced Plastics and Composites*, 2002; 21(9): 775-805.
- Hughes TJR, Taylor RL, Kanoknukulchai W. A simple and efficient finite element for plate bending. *International Journal for Numerical Methods in Engineering*, 1977; 11: 1529-1543.
- Hughes TJR, Cohen M, Haroun M. Reduced and selective integration techniques in finite element analysis of plates, *Nuclear Engineering and Design*, 1978; 46: 203-222.
- Hughes TJR, Cohen M. The "Heterosis" Finite Element for Plate Bending. *Computer and Structures*, 1978; 9: 445-450.
- Lo KH, Cristensen RM, Wu EM. A High-Order Theory of Plate Deformation, Part 1: Homogeneous Plates. *Journal of Applied Mechanics*, 1977; 44(4): 663-668.
- Lo KH, Cristensen RM, Wu EM. A High-Order Theory of Plate Deformation, Part 2: Laminated Plates. *Journal of Applied Mechanics*, 1977; 44(4): 669-676.
- Prathap G. A field-consistency approach to plate elements. *Structural Engineering and Mechanics*, 1997; 5(6): 853-865.
- Reddy JN, Averill, RC. Advances in the Modelling of Laminated Plates. *Computing Systems in Engineering*, 1991; 2(5/6) : 541-555.
- Reddy, JN. *Mechanics of Laminated Composite Plates and Shells: Theory and Analysis*, 2<sup>nd</sup> ed., Boca Raton, FL: CRC Press, 2004.
- Reddy JN, Wang CM. An Overview of the Relationships between Solutions of the Classical and Shear Deformation Plate Theories. *Composites Science and Technology*, 2000; 60: 2327-2335.
- Reddy JN. On Refined Computational Models of Composite Laminates, *International Journal for Numerical Methods in Engineering*, 1989; 27: 361-382.
- Sheikh AH, Chakrabarti A. A new plate bending element based on higher-order shear deformation theory for the analysis of composite plates. *Finite Elements in Analysis and Design*, 2003; 39: 883- 903.

- Singh G, Rao GV. A Discussion on Simple Third-Order Theories and Elasticity Approaches for Flexure of Laminated Plates. *Structural Engineering and Mechanics*, 1995; 3(2): 121-133.
- Zienkiewicz OC, Taylor RL, Too JM. Reduced integration technique in general analysis of plates and shells. *International Journal for Numerical Methods in Engineering*, 1971; 3: 275-290.